Available online at www.sciencedirect.com
SCIENCE DIRECT
Bioorganic & Medicinal Chemistry 14 (2006) 5384–5388
Bioorganic & Medicinal Chemistry

Evaluation of mismatch-binding ligands as inhibitors for Rev–RRE interaction

Kazuhiko Nakatani,[a,b,*] Souta Horie,[a] Yuki Goto,[a] Akio Kobori[a,†] and Shinya Hagihara[a,‡]

[a]*Department of Synthetic Chemistry and Biological Chemistry, Faculty of Engineering, Kyoto University, Kyoto 615-8510, Japan*
[b]*The Institute of Scientific and Industrial Research (SANKEN), Osaka University, 8-1 Mihogaoka, Ibaraki 567-0047, Japan*

Received 18 January 2006; revised 20 March 2006; accepted 21 March 2006
Available online 5 April 2006

Abstract—Drugs targeting the stem-loop IIB of Rev responsible element (RRE) of HIV-1 mRNA are potential therapeutic agents for HIV-1 infection. The stem loop is characterized by an internal loop consist of consecutive G-G and G-A mismatches, which is the single binding site for Rev protein for nuclear export of viral mRNA. We report here that ligands binding to G-G and G-A mismatches in duplex DNA also bind to the internal loop in competition with Rev peptide and lead to the dissociation of pre-formed Rev–RRE complex in a model system.

1. Introduction

The Rev responsible element (RRE) of HIV-1 mRNA is a large RNA structure residing within the region that codes envelope proteins[1] and serves as a docking site for the Rev protein.[2,3] Binding of the Rev protein to RRE induces the nuclear export to the cytoplasm of unspliced or partially spliced viral mRNA. Interference in the formation of the Rev–RRE complex inhibits nuclear transport of the unspliced mRNA, eventually causing suppression of HIV-1 replication. An internal loop in stem-loop IIB of RRE has been identified as a single high-affinity site for the Rev binding[4,5] (Chart 1). Thus, small molecular ligands that bind to the loop in competition with Rev protein are potential therapeutic agents for treating HIV-1 infection.[6–8]

However, the design of RNA targeting molecules still remained to be a challenge in medicinal chemistry because of the complicated RNA secondary and tertiary structures.[9–11] We have discovered a novel class of compounds that bind selectively to the mismatched base pair in duplex DNA. The stem-loop IIB of HIV-1 RRE is characterized by an internal loop consisting of two consecutive mismatched base pairs, one a G-G mismatch and the other a G-A mismatch. These non-Watson–Crick base pairs have been shown to be responsible for the Rev binding. We here report that naphthyridine dimer (**ND**)[12,13] and naphthyridine–azaquinolone (**NA**)[14,15] which bind to the G-G and G-A mismatches in duplex DNA, respectively, are the potential candidates of drug lead that inhibits the Rev–RRE interaction (Chart 2).

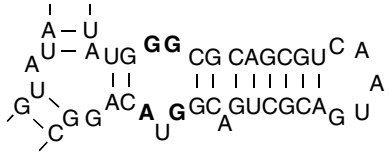

stem-loop IIB of HIV-1 RRE

Chart 1. A structure of stem-loop IIB of HIV-1 mRNA.

2. Results and discussion

We first qualitatively evaluated the binding of **ND** and **NA** to various RNA structures using surface plasmon resonance (SPR) assay with the sensors carrying **ND**

Keywords: RNA recognition; Inhibitors; Drug design; HIV-1 RRE.
* Corresponding author. Tel.: +81 6 6879 8455; fax: +81 6 6879 8459; e-mail: nakatani@sanken.osaka-u.ac.jp
† Present address: Department of Polymer Science and Engineering, Kyoto Institute of Technology, Matsugasaki, Sakyo-ku, Kyoto 606-8585, Japan.
‡ Present address: RIKEN (The Institute of Physical and Chemical Research), 2-1 Hirosawa, Wako-shi, Saitama 351-0198, Japan.

0968-0896/$ - see front matter © 2006 Elsevier Ltd. All rights reserved.
doi:10.1016/j.bmc.2006.03.038

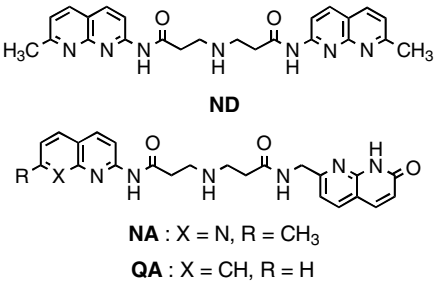

Chart 2. Structures of ligands used in these studies.

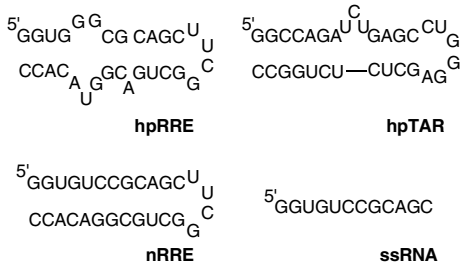

Chart 4. RNAs used in these studies and their possible secondary structures.

and **NA** on the surfaces. **ND** was immobilized as **aminolink-ND** at the secondary nitrogen by way of a short aminoalkyl linker onto the surface of carboxymethyl dextran of a CM5 sensor chip (BIAcore) (Chart 3).[12] **NA** was immobilized as a form of amino-linked dimer (**aminolink-NA**) to increase a surface density of the ligand,[15] because the **NA**-binding to a G-A mismatch in RNA was anticipated to be weaker than the **ND**-binding to a G-G mismatch based on their bindings to the mismatches in duplex DNA. Using the **ND**-immobilized sensor, a strong SPR response was observed for a hairpin RNA (**hpRRE**) (Chart 4) representing the stem-loop IIB of HIV-1 RRE (Fig. 1a). In contrast, a completely matched hairpin RNA (**nRRE**), which lacked an internal loop consisting of the G-G and G-A mismatches, did not bind to the **ND**-immobilized sensor surface. Very weak binding was observed for a single stranded RNA (**ssRNA**) and a hairpin RNA representing TAR RNA of HIV-1 (**hpTAR**) containing the r(UCU) bulge. SPR analyses with **NA**-immobilized surfaces showed a strong SPR response for **hpRRE**, whereas virtually no responses for other three RNAs (Fig. 1b). These experiments demonstrated that both **ND** and **NA** did not bind to a completely matched RNA duplex, r(UUCG) and r(CUGGGA) hairpin loops, and a r(UCU) bulge. Thus, the internal loop consisting of the G-G and G-A mismatches in **hpRRE** is most likely the binding site of both **ND** and **NA**.

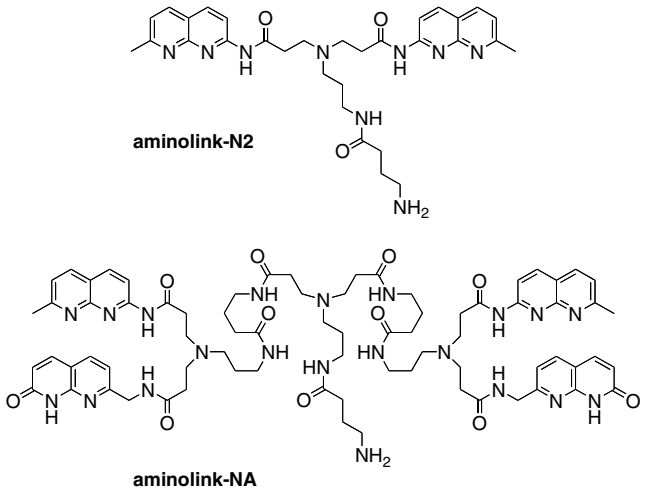

Chart 3. Structures of **aminolink-ND** and **aminolink-NA** used for the immobilization of **ND** and **NA**, respectively, onto the SPR sensor surface.

Separate experiments showed that **ND**-binding to the G-G mismatches in duplex RNA was favorable for those flanked by a single nucleotide bulge. (Table 1) The increase of T_m (ΔT_m) of G-G mismatch RNA duplex was 4.8 °C, whereas it increased up to 9.1 °C when the G-G mismatch was flanked by a single uridine and adenine bulge. Since the single uridine and adenine bulge in RNA duplex was not the site of the **ND** binding, it is most likely that structural perturbation on the G-G mismatch by the neighboring nucleotide bulge favorably affected the **ND**-binding to the G-G mismatch in RNA duplexes. The RNA duplex is known to have A-form, which has a deep major groove compared to that of B-form DNA duplex. **ND** binds to the G-G mismatch from the major groove side of DNA duplex. Thus, the single nucleotide bulge flanking the G-G mismatch may loosen the deep major groove to facilitate the **ND**-binding.

The binding of **ND** and **NA** to the stem-loop IIB of RRE was examined with respect to the structure of the heterocycles in the ligand. We measured the difference in the absorption spectra of ligands between the absence and presence of **hpRRE**. The absorption of unbound **ND** at 320 nm decreased with a concomitant bathochromic shift as indicated by an increased absorption at 345 nm (Fig. 2a). Similar changes in the UV spectra were observed for **NA** with a decreased efficiency. Bathochromic shifts of the ligand absorptions suggested the stacking interaction of bound **ND** and **NA** with the neighboring bases in **hpRRE**. In contrast, a ligand, aminoquinoline–azaquinolone (**QA**), which did not bind to the G-G and G-A mismatches in duplex DNA,[14] showed little absorption change in the spectra. A complete loss of binding as observed for **QA** suggested an important role of 2-aminonaphthyridine for the binding to **hpRRE**. The UV absorption change of these ligands in the presence of **nRRE** was quite small with virtually no bathochromic shift, strongly suggesting that the internal loop in **hpRRE** would be the site of binding of **ND** and **NA** (Fig. 2b).

Having the data indicating the binding of **ND** and **NA** to **hpRRE**, we investigated competitive binding of these molecules with the Rev model peptide 5,6TAMRA-TRQARRNRRRRWRERQRAAAAK-amide (**tamRev**) by fluorescence anisotropy displacement assay.[6,16] The peptide consisted of an arginine-rich motif ($Rev_{34–50}$) and an alanine-rich sequence, and was previously shown to interact with high affinity to RRE stem-loop IIB.[6,17]

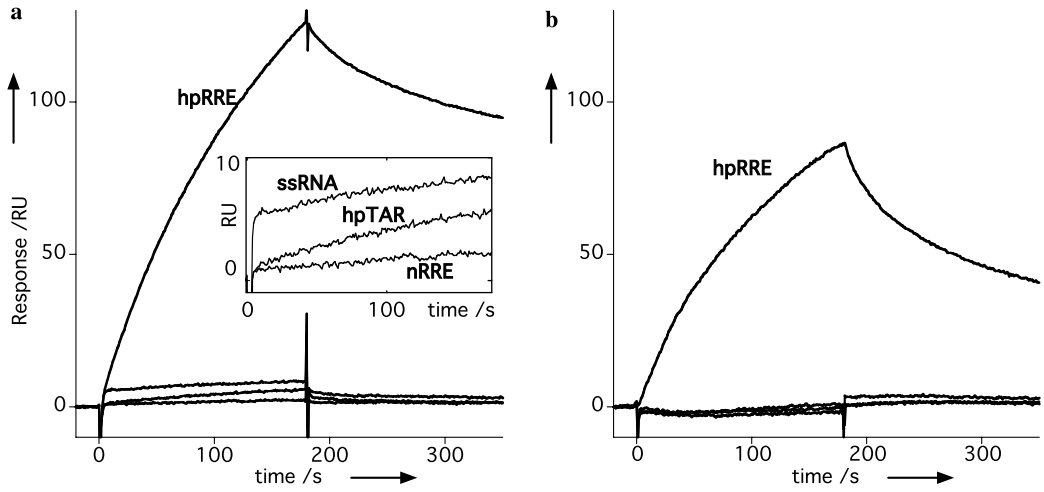

Figure 1. SPR assays of RNA-binding to the ligand-immobilized sensor surfaces. RNA sample (**hpRRE**, **nRRE**, **hpTAR**, and **ssRNA**, each 100 nM) in 10 mM HEPES and 150 mM NaCl was heat denatured, folded by slow cooling, and applied to the sensor for 180 s with a flow rate of 30 μL/min. (a) **ND**-immobilized sensor surface. Inset: expansion of the responses from 0 to 10 RU. The amount of **ND** immobilized on the surface was 370 RU. (b) **NA**-immobilized sensor surface. The amount of **NA** immobilized on the surface was 1900 RU.

Table 1. Melting temperature (T_m) of RNA in the absence of **ND**

RNA sequence	T_m (°C)		ΔT_m (°C)
	RNA	RNA + **ND**	
5′-r(CUAACGGAAUG)-3′ 3′-r(GAUUGCCUUAC)-5′	48.7	47.9	−0.8
5′-r(CUAAC**G**GAAUG)-3′ 3′-r(GAUUG**G**CUUAC)-5′	33.5	38.3	4.8
5′-r(CUAAC**G** GAAUG)-3′ 3′-r(GAUUG**C** CUUAC)-5′ **U**	36.0	36.5	0.5
5′-r(CUAAC**G** GAAUG)-3′ 3′-r(GAUUG**C** CUUAC)-5′ **A**	35.1	35.2	0.1
5′-r(CUAAC**G** GAAUG)-3′ 3′-r(GAUUG**G** CUUAC)-5′ **U**	30.6	39.7	9.1
5′-r(CUAAC **G**GAAUG)-3′ 3′-r(GAUUG **G**CUUAC)-5′ **U**	29.3	38.1	8.8
5′-r(CUAAC**G** GAAUG)-3′ 3′-r(GAUUG**G** CUUAC)-5′ **A**	26.4	35.0	8.6
5′-r(CUAAC **G**GAAUG)-3′ 3′-r(GAUUG **G**CUUAC)-5′ **A**	26.8	35.4	8.6

The UV–melting curves were measured for duplexes (4 μM) in 10 mM sodium cacodylate buffer (pH 7.0) containing 100 mM NaCl in the absence and presence of ND (100 μM). Temperature was increased at a rate of 1 °C/min.

The N-terminal was fluorescently labeled with 5,6-TAMRA, whereas C-terminal was amidated. Upon addition of **hpRRE**, fluorescence anisotropy of **tamRev** (100 nM) increased markedly with increasing concentrations of **hpRRE** up to 160 nM, above which anisotropy exhibited a plateau, indicating formation of a complex (**tamRev**–**hpRRE**) (Fig. 3a). Using a nonlinear regression analysis of the binding curve reported earlier,[6,18] the dissociation constant of the **tamRev**–**hpRRE** complex was determined to be 5.6 nM. To examine inhibitory activities of the ligands on the formation of the **tamRev**–**hpRRE** complex, we measured the decrease in fluorescence anisotropy of a pre-formed **tamRev**–**hpRRE** complex upon titrating with the ligands. A release of bound **tamRev** from the complex by ligand displacement resulted in a decrease of fluorescence anisotropy. Upon titrating the **tamRev**–**hpRRE** complex with **ND**, **NA**, and neomycin B, a decrease in fluorescence anisotropy was

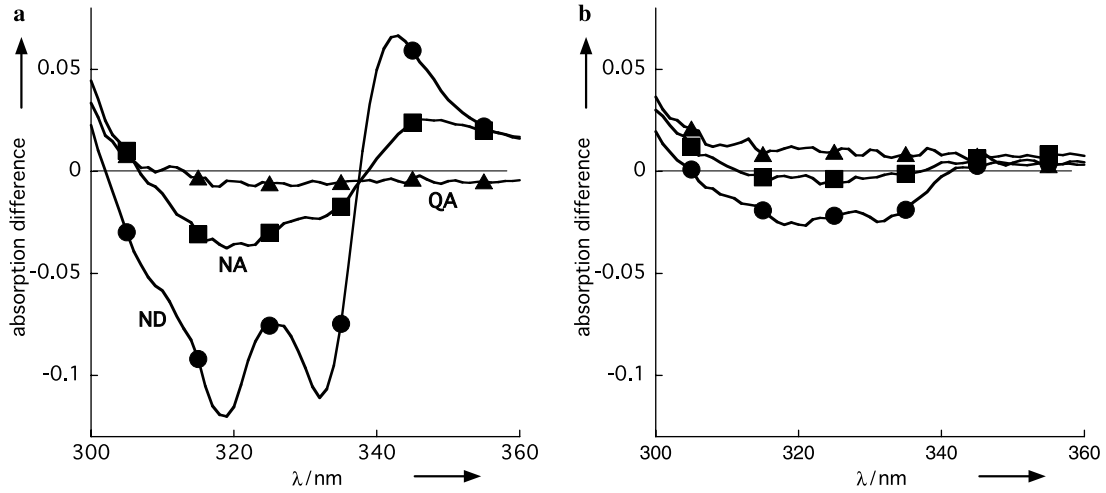

Figure 2. Difference UV spectra of ligands (20 μM) in the presence of (a) **hpRRE** (2 μM) and (b) **nRRE** (2 μM) in sodium phosphate (pH 7.0) containing EDTA (1 mM) and NaCl (100 mM). Key: **ND** (circle); **NA** (square); **QA** (triangle).

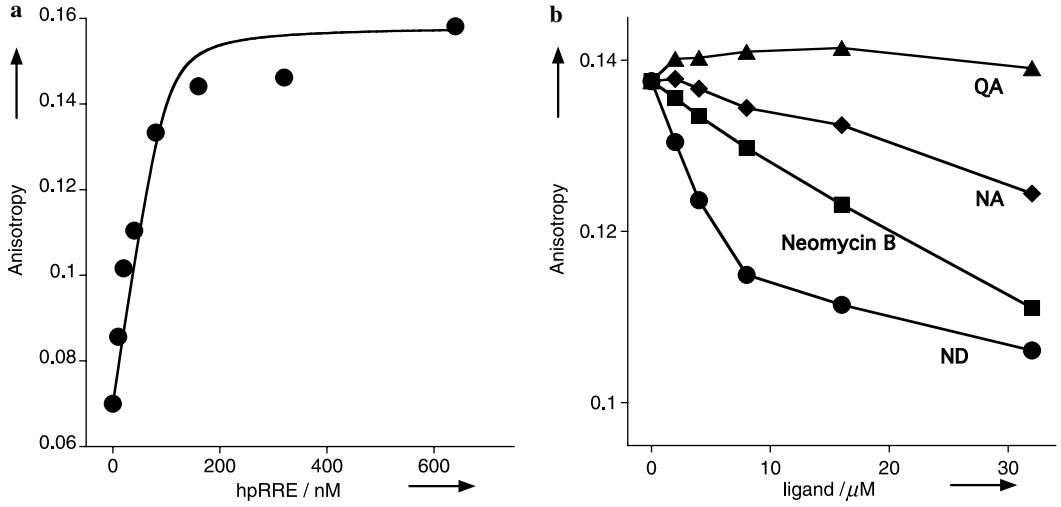

Figure 3. Fluorescence anisotropy assay. (a) A change of fluorescence anisotropy of **tamRev** (100 nM) (circle) titrated with **hpRRE**. Concentrations of **hpRRE** were 0, 10, 20, 40, 80, 160, 320, and 640 nM. The solid line represents a calculated binding curve obtained by a nonlinear regression analysis of the raw data. (b) Decreases of anisotropy by titrating the pre-formed complex between **hpRRE** (100 nM) and **tamRev** (100 nM) with ligands. Ligand concentrations were 0, 2, 4, 8, 16, and 32 μM. Key: **ND** (circle), **NA** (diamond), neomycin B (square), and **QA** (triangle).

observed, but not with **QA** (Fig. 3b). The dissociation of the **tamRev**–**hpRRE** complex was induced by **ND** much more efficiently than by neomycin B and **NA**.

3. Conclusion

The data reported here showed that (1) ligands binding to G-G and G-A mismatches in duplex DNA could also bind to a stem-loop IIB of RRE and (2) **ND** showed a stronger inhibitory activity for **tamRev**–**hpRRE** formation than neomycin B. While the precise mode of the binding as well as the binding stoichiometry of **ND** could not be determined by SPR and mass spectrometry, **ND** and **NA** were found useful to capture HIV-1 RRE when these molecules were immobilized on the surface. In addition, these results suggested that structural optimization of **ND** and **NA** toward the binding to the internal loop may lead molecules showing potent inhibitory activities against Rev–RRE binding.

4. Experimental

4.1. Substrates

All RNAs were purchased from PROLIGO with HPLC purification. 5,6-TAMRA-labeled peptide model was custom synthesized by Biosource International Inc. (Camarillo, California) with a purity of >95%.

4.2. General procedure for SPR-binding experiments

All measurements were carried out at 25 °C in a continuous flow of HBS-N buffer (10 mM HEPES, pH 7.4) containing NaCl (150 mM) at a flow rate of

30 μL/min. RNA samples (0.1 μM) in HBS-N buffer were heat denatured, folded by slow cooling, and injected into the sensor for 3 min to analyze the association to the surface. Then, the dissociation of the bound RNA to the surface was analyzed by injecting buffer only.

4.3. UV measurements

All UV measurements were carried out with SHIMADZU UV-2550 (Kyoto, Japan) at 25 °C.

4.3.1. Sample preparation. hpRRE, **hpTar**, **ssRNA**, and **nRRE** (2 μM) were denatured at 90 °C and cooled down slowly to a room temperature in a buffer (3.75 mM Na-phosphate, pH 7.0, 100 mM NaCl, 1.0 mM EDTA). A solution of ligand (20 μM) was added to the solution and left for 1 h at 25 °C. UV spectra were measured for each ligand with or without RNA. The difference UV spectra were obtained by subtracting the data in the presence of RNA from the data in the absence of RNA.

4.4. Fluorescence anisotropy assay

Fluorescence Anisotropy assays were carried out with a Beacon2000 system (Invitrogen) at 25 °C.

4.4.1. tamRev–hpRRE binding. hpRRE was denatured at 90 °C and cooled down slowly to a room temperature in a buffer (30 mM HEPES, pH 7.5, 10 mM Na-phosphate, pH 7.5, 100 mM KCl, 10 mM NH_4OAc, 0.1% Nonidet NP-40, 10 mM guanidine·HCl, 2 mM $MgCl_2$, 20 mM NaCl, 0.5 mM EDTA). To the solution of variable concentrations of **hpRRE** (10, 20, 40, 80, 160, 320, and 640 nM), **tamRev** (100 nM) was added and left for 12 h at 25 °C. Fluorescence anisotropy of the complex was measured with Beacon2000 at 25 °C. Average read cycles for the measurements were set to 10. The range control was auto.

4.4.2. Inhibition assay. tamRev–hpRRE complex was prepared by mixing 100 nM of each **tamRev** and **hpRRE** in a buffer as described above. A varing concentration of ligand (2, 4, 8, 16, and 32 μM) was added to the solution of **tamRev–hpRRE**, and the whole solution was left at 25 °C for 12 h. Fluorescence anisotropy was measured as above.

4.4.3. Curve fitting. Non-linear regression analysis for the **tamRev–hpRRE** formation was carried out by SigmaPlot2001 by using the equation for the 1:1 binding as shown below:

$$A_{\mathrm{obs}} = (A_{\max} - A_0) \cdot \alpha + \mathrm{A}_0,$$

$$\alpha = \frac{([\mathrm{Rev}]_0 + [\mathrm{RRE}]_0 + K_{\mathrm{d}}) \pm \sqrt{([\mathrm{Rev}]_0 + [\mathrm{RRE}]_0 + K_{\mathrm{d}})^2 - 4 \cdot [\mathrm{Rev}]_0 \cdot [\mathrm{RRE}]_0}}{2 \cdot [\mathrm{Rev}]_0},$$

where A_0 and $A_{\max}$ are anisotropy observed at 0 and 600 nM of **hpRRE**. $[\mathrm{Rev}]_0$ and $[\mathrm{RRE}]_0$ are the total concentration of each. K_{d} is the dissociation constant, whereas α is the molar fraction of Rev–RRE complex against $[\mathrm{Rev}]_0$.

Acknowledgment

Authors thank Dr. Fumie Takei for the experimental assistance.

References and notes

1. Pollard, V. M.; Malim, M. H. *Annu. Rev. Microbiol.* **1998**, *52*, 491–532.
2. Malim, M. H.; Böhnlein, S.; Hauber, J.; Cullen, B. R. *Cell* **1989**, *58*, 205–214.
3. Daly, T. J.; Cook, K. S.; Gray, G. S.; Maione, T. E.; Rusche, J. R. *Nature* **1989**, *342*, 816–819.
4. Bartel, D. P.; Zapp, M. L.; Green, M. R.; Szostak, J. W. *Cell* **1991**, *67*, 529–536.
5. Iwai, S.; Pritchard, C.; Mann, D. A.; Karn, J.; Gait, M. J. *Nucleic Acids Res.* **1992**, *20*, 6465–6472.
6. Luedtke, N. W.; Tor, Y. *Angew. Chem., Int. Ed.* **2000**, *39*, 1788–1790.
7. Kirk, S. R.; Luedtke, N. W.; Tor, Y. *J. Am. Chem. Soc.* **2000**, *122*, 980–981.
8. Hendrix, M.; Priestley, E. S.; Joyce, G. F.; Wong, C.-H. *J. Am. Chem. Soc.* **1997**, *119*, 3641–3648.
9. Zaman, G. J. L.; Michiels, P. J. A.; van Boeckel, C. A. A. *Drug Discovery Today* **2003**, *8*, 297–306.
10. Gallego, J.; Varani, G. *Acc. Chem. Res.* **2001**, *34*, 836–843.
11. Tok, J. B. H.; Bi, L. R.; Saenz, M. *Bioorg. Med. Chem. Lett.* **2005**, *15*, 827–831.
12. Nakatani, K.; Sando, S.; Saito, I. *Nat. Biotechnol.* **2001**, *19*, 51–55.
13. Nakatani, K.; Sando, S.; Kumasawa, H.; Kikuchi, J.; Saito, I. *J. Am. Chem. Soc.* **2001**, *123*, 12650–12657.
14. Hagihara, S.; Kumasawa, H.; Goto, Y.; Hayashi, G.; Kobori, A.; Saito, I.; Nakatani, K. *Nucleic Acids Res.* **2004**, *32*, 278–286.
15. Nakatani, K.; Hagihara, S.; Goto, Y.; Kobori, A.; Hagihara, M.; Hayashi, G.; Kyo, M.; Nomura, M.; Mishima, M.; Kojima, C. *Nat. Chem. Biol.* **2005**, *1*, 39–43.
16. Luedtke, N. W.; Tor, Y. *Biopolymers* **2003**, *70*, 103–119.
17. Lacourciere, K. A.; Stivers, J. T.; Marino, J. P. *Biochemistry* **2000**, *39*, 5630–5641, With a short RRE construct, neomycin showed K_{i} value of 2 μM for inhibition of Rev binding. The highest affinity site of RRE for neomycin-binding ($K_{\mathrm{d}} = 0.24$ μM) was not disruptive to Rev-binding.
18. Sevenich, F. W.; Langowski, J.; Weiss, V.; Rippe, K. *Nucleic Acids Res.* **1998**, *26*, 1373–1381.